JP0350358

3.31 Measurement of Total Cross-Sections of Natural Dy, In and Cu at the Pohang Neutron Facility

Guinyun Kim,[*] Rachid Machrafi, Hossain Ahmed, and Dongchul Son
Institute of High Energy Physics, Kyungpook National University,
1370 Sankyuk-Dong, Puk-Gu, Daegu 702-701, Korea

Vadim Skoy,[‡] Young Seok Lee, Hengsik Kang, Moo-Hyun Cho, In Soo Ko, and Won Namkung
Pohang Accelerator Laboratory, Pohang University of Science and Technology,
San 31 Hyoja–Dong, Nam–Gu, Pohang 790 – 784, Korea

The Pohang Neutron Facility consists of an electron linear accelerator, a water-cooled Ta target, and an 11-m time-of-flight path which has been constructed for nuclear data production. It has been equipped with a new four-position sample changer controlled remotely by a CAMAC data acquisition system, which allows simultaneous accumulation of the neutron time of flight spectra from 4 different detectors. The neutron total cross-sections of natural Dy, In and Cu were measured in the neutron energy range from 0.1 eV to 100 eV by using the neutron time of flight method with the new data acquisition system. A ^{6}LiZnS(Ag) glass scintillator was used as a neutron detector and metallic plates of natural Dy, In and Cu samples were used for the neutron transmission measurement. The neutron flight path from the water-cooled Ta target to the neutron detector was 10.81 ± 0.02 m. The background level was determined by using notch-filters of Co, Ta, and Cd sheets. In order to reduce the gamma rays from Bremsstrahlung and those from neutron capture, we employed a neutron-gamma separation system based on their different pulse shapes. The present measurements are in general agreement with the evaluated data in ENDF/B-VI. The resonance parameters of the Dy and In isotopes were extracted from the transmission data and compared with the previous ones.

I. INTRODUCTION

Pulsed neutrons based on an electron accelerator (linac) are a powerful tool to measure the energy dependence of cross-sections with high resolution by using time of flight (TOF). The Pohang Neutron Facility (PNF) was proposed in 1997 and constructed at the Pohang Accelerator Laboratory on December 1998 [1]. It consists of a 100-MeV electron linac, water-cooled Ta neutron producing target, and an 11-m-long evacuated flight vertical tube leading to the detector location. Neutrons are produced by the bremsstrahlung process from a tantalum radiator. The facility details of PNF are described elsewhere [2].

The neutron total cross-section is used in nuclear data extraction as well as in nuclear applications such as design of nuclear plants. A few measurements of the neutron total cross-sections for Dy have been reported below 100 eV. Moore [3] and Okamoto [4] measured the total cross-sections of Dy in the thermal neutron energy region by the transmission method. Sailor et al. [5] reported the neutron total cross-sections in the energy range from 0.07 to 20 eV measured with a crystal spectrometer. Brunner et al. [6] obtained the total cross-sections in the energy range from 0.015 eV to 2.5 eV with a fast-chopper installed in a thermal reactor. Knorr et al. [7] reported the total cross-sections in the energy region below 3.2×10^{-3} eV. Recently, Cho et al. [8] measured the total cross-sections of Dy in the energy region from 0.002 to 100 keV by using the neutron TOF method with a 46 MeV electron linac of the Research Reactor Institute, Kyoto University. However, there exist discrepancies among the measurements, especially in the resonance energy region.

The Brookhaven fast chopper Seth has been used to measure the transmission ratio for different elements [9]. The total cross-sections of Cu and other elements have been used to determine the nuclear potential radius and to investigate the predictions of the nuclear optical model. At the ORELA neutron facility, Pandey et al. have measured the total cross-sections and resonance parameters of [63, 65]Cu [10] in resonance energy range.

The early studies of transmission of In are reported in Refs. 11-13. Harvey et al. has measured the transmission of enriched In in the neutron energy range higher than 3 eV and determined the resonance parameters [14]. In the work of Bacher et al. [15], to establish more accurately the energy of the resonance above 1.0 eV, they measured the transmission rate covering the energy range from 0.75 to 10 eV, and determined that the resonance energy was between 1.29 and 1.43 eV; later it was defined at 1.35 eV. By studying low-energy neutrons, Havens et al. determined the first resonance at 1.44 eV and two others, one at 3.8 eV and the other at 8.6 eV [16]. Bacher et al. also investigated the slow neutron energy region of Rh and In, but the poor energy resolution at that time didn't allow them to identy the energy resonance around 1 eV which was fixed with a probable error of about 10%. Later, Boyce and McDaniel fixed this resonance at 1.44 and identified two others, one at 3.7 and the other at 9.0 eV [17]. Using the Nevis synchrocyclotron, Hacken et al. investigated the resonance parameters [18]. The most recent work on In was reported by Franke et al. [19]. The work was performed for energies of 25 eV up to 500 eV at the Los Alamos Neutron Scattering Center. In this study, 47 unreported resonances were observed; also, new data was obtained for the resonance parameters by combining the total and the capture cross-sections.

The measured result was compared with the evaluated data in ENDF/B-VI [20]. The resonance parameters for Dy isotopes ([161,162,163]Dy) were determined from the fitting of transmission data by using the Multilevel R-Matrix code SAMMY [21] and compared with Mughabghab's data [22].

II. EXPERIMENTAL ARRANGEMENT

The experimental arrangement for the transmission measurements is shown in Fig. 1. The target is located in the position where the electron beam hits its center. To reduce the gamma-flash generated by the electron burst in the target, this one was placed 55 mm away from the center of the neutron guide. The target was composed of ten Ta plates with a diameter of 4.9 cm and an effective thickness of 7.4 cm [23]. There was a 0.15-cm water gap between Ta plates in order to cool the target effectively. The housing of the target was made of titanium. This target was set at the center of a cylindrical water moderator contained in an aluminum cylinder with a thickness of 0.5 cm, a diameter of 30 cm, and a height of 30 cm. The water level in the moderator was 3 cm above the target surface, which was decided based on a measurement of the thermal neutron flux. The measurement was also compared with the Monte Carlo N-Particle (MCNP) transport code [24].

The neutron guide tubes were constructed of stainless steel with two different diameters, 15 cm and 20 cm, and were placed perpendicularly to the electron beam. The neutron collimation system was mainly composed of H_3BO_3, Pb and Fe collimators, which were symmetrically tapered from a 10-cm diameter at the beginning, to a 5-cm diameter in the middle position where the sample changer was located, to an 8-cm diameter at the end of guide tube where the neutron detector was placed. There was 1.8-m-thick concrete between the target and the detector room.

The physical parameters of the samples used in the experiment are given in Table 1. A set of notch filters of Co, Ta, and Cd plates with thickness of 0.5 mm, 0.2 mm, and 0.5 mm, respectively, was also used for the background measurement and the energy calibration. The transmission samples were placed at the midpoint of the flight path and were cycled into the neutron beam by using the automatic sample changer with four sample positions.

Table 1. Physical parameters of the samples used in the experiment.

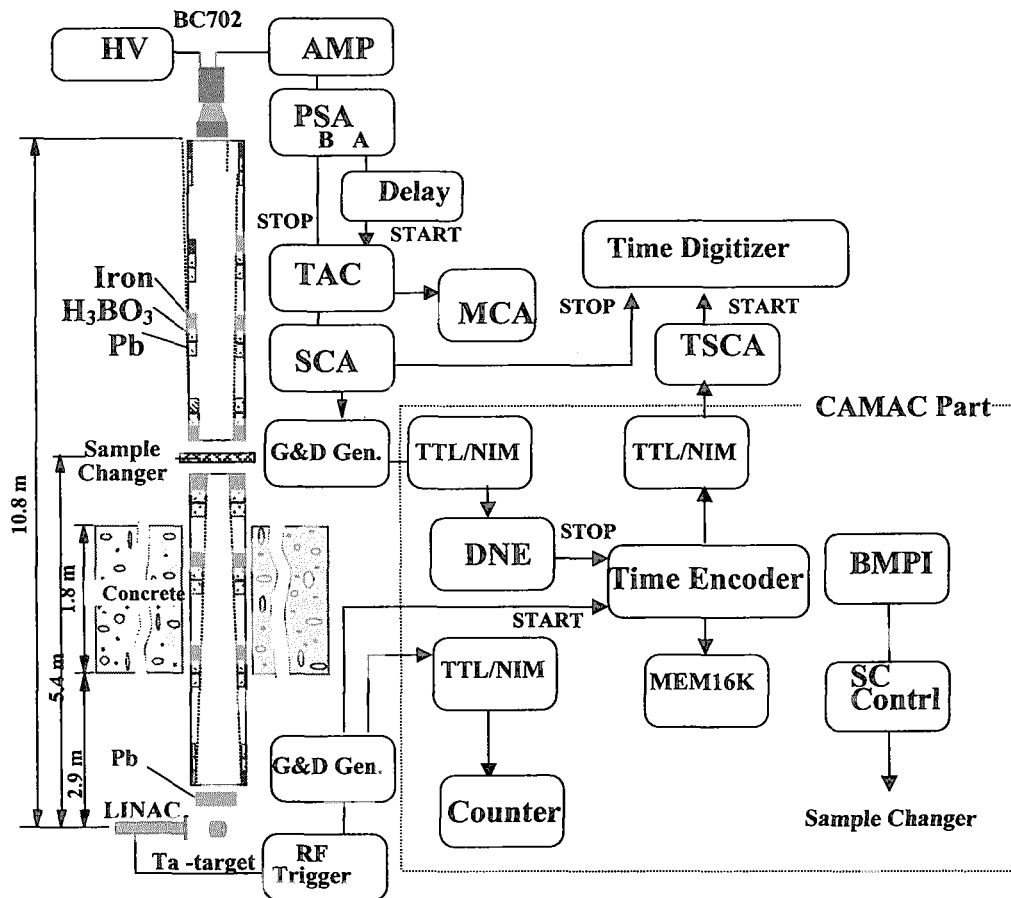| Sample	Purity (%)	Size (cm^2)	Thickness (mm)	Weight (g)
Dy	99.90	10×10	0.5	42.76
In	99.99	10×10	0.2	9.84
Cu	99.96	10×10	1.5	134.4

Fig.1. Experimental setup for the transmission measurements.

The neutron detector was located at a distance of 10.81 m from the photo-neutron target. A ^{6}Li-ZnS(Ag) scintillator BC702 from Bicron (Newbury, Ohio) with a diameter of 127 mm and a thickness of 15.9 mm mounted on an EMI-93090 photomultiplier was used as a detector for the neutron TOF spectrum measurement. This scintillator consists of a matrix of a lithium compound enriched to 95% ^{6}Li dispersed in a fine ZnS(Ag) phosphor powder. The detection process employs the nuclear reaction ^{6}Li $(n,\alpha)^3$H in which the resulting α - particle and ^{3}H produce scintillations upon interacting with the ZnS(Ag).

During the experiment, the electron linac was operated with a repetition rate of 10 Hz, a pulse width of 1.0 μs and the electron energy of 60 MeV. The peak current in the beam current monitor located at the end of the second accelerator section is above 50 mA, which almost is the same as that in the target.

III. DATA TAKING AND ANALYSIS

Figure 1 shows the configuration of the data acquisition system used in our measurement. Two different data acquisition systems were used for the neutron TOF spectra measurements: one for the NIM-based system and the other for the CAMAC-based system. The main purpose of the NIM-based system was neutron-gamma separation and the parallel accumulation of the neutron TOF spectra if necessary. The process of neutron-gamma separation was described in details elsewhere [25].

The dynode signal from a BC702 scintillator was connected through an ORTEC-571 amplifier (AMP) to an ORTEC-552 pulse-shape analyzer (PSA) for use in neutron-gamma separation. A fast NIM signal from the "A" output of the PSA was delayed by 60 ns and used as the start signal for an ORTEC-567 time-to-amplitude converter (TAC). The "B" output signal from the PSA was used as the stop signal for the TAC. One of TAC outputs was connected to an ORTEC-550A single channel analyzer (SCA), and the other output signal was fed to a multi-channel pulse-height analyzer (MCA) for neutron-gamma separation. The output signal of the SCA was used as stop signals for a 150-MHz Turbo MCS (Time Digitizer) and for a time encoder of the CAMAC-based system for the neutron TOF spectra measurement. The output of the SCA was sent to an ORTEC-416A gate and delay generator (G&D Gen.) and a TTL/NIM module in order

to form the proper signal for the CAMAC system. This output signal was connected to a time encoder through a detector number encoder (DNE). The DNE allowed data taking from up to 4 detectors simultaneously. The time encoder had 4096 channels and a minimal dwell time of 0.5 μs. MEM16K is a memory of 16K capacity and collected the TOF spectra during the measurement.

The 10-Hz RF trigger signal for the modulator of the electron linac was connected to a G&D Gen.; one of output signals was used as the start signal for both the time digitizer and the time encoder, and the other output was sent to the counter through a TTL/NIM converter. The remote control signal from the TTL/NIM was used as the start pulse for the time digitizer for parallel data accumulation. In distinction with the direct use of the start pulse from the RF trigger for the time digitizer, this scheme temporarily interrupts the start pulse sequence while the sample changer moves. The counter has 4 independent inputs, as well as the relevant displays for data and control signals. It is used to accumulate the monitor counts for each position of the sample changer and to control the duration of sample exposure.

Block BMPI sends a request to the sample changer control (SC Contr.) block to change the sample and interrupts the measurement until the next sample reaches its position. The SC Contr. block can be operated automatically (normal mode), as well as manually (manual mode). In the normal mode, it is controlled by software via the BMPI. In the manual mode, one can move the sample changer to any desired position by pressing the relevant knob on the front panel of that block. This mode is usually applied during sample downloading.

The CAMAC part is controlled by PC software via an interface card and crate controller (not shown in Fig. 1). The program sets and controls the following parameters:

- the numbers and quantity of actual detectors used in the measurement;
- the actual number of TOF channels and dwell time for each detector (may be different);
- the duration of the exposition for each sample as the number of starts from the linac.

It also sets the number of full turnovers of the SC and provides a data record from the MEM16K to the relevant files for future processing. Parallel data acquisition with both the Turbo-MCS system and the CAMAC system may be used if one desires to optimize the dwell time for different regions of the TOF spectra. For example, the CAMAC time encoder dwell time may be set to 0.5 μs to get good energy resolution in the high-energy part of the TOF spectra while the simultaneous setting for the Turbo-MSC might be 1.5 μs to approach, say, 1 meV in the low-energy region of the TOF spectra. A command file written in special script language synchronizes the CAMAC and the Turbo-MCS.

We could estimate the background level by using resonance energies of the neutron TOF spectra of notch-filters of Co, Ta and Cd. The magnitude of the background level was interpolated between the black resonances by using the fitting function $F(I) = a + b\,I$, where a and b are constants and I is the channel number of the time digitizer. In the transmission measurements, we have taken data with sample in and out (open beam) periodically. Total data taking times for sample and open runs of Dy, In, and Cu are 18, 21.5, and 31.25 hours and 16, 21.5 and 31.25 hours, respectively. The net neutron TOF spectra for the sample runs and the open runs for each sample are shown in Fig. 2 together with the estimated background level indicated by dash line. The neutron energy E in eV corresponding to each channel I in the TOF spectrum is derived from the relation; $E = \{72.3 \times L /(I - I_0) \times W\}^2$, where $L = 10.81 \pm 0.02$ m is the neutron flight path, W = 0.5 μs is the channel width of the time digitizer, and I_0 is the channel of TOF=0 when the neutron burst was produced. In this experiment we found I_0 equals to 5 channels.

The neutron total cross-section is determined by measuring the transmission of neutrons through the sample. The transmission rate of neutrons at the i-th group energy E_i is defined as the fraction of incident neutrons passing through the sample compared to that in the open beam. Thus, the neutron total cross-section is related to the neutron transmission rate $T(E_i)$ as follows:

$$\sigma(E_i) = -\frac{1}{\sum\limits_j N_j} \ln T(E_i),$$
(1)

$$T(E_i) = \frac{[I(E_i) - IB(E_i)]/M_I}{[O(E_i) - OB(E_i)]/M_O},$$
(2)

where N_j is the atomic density per cm^2 of the j-th isotope in the sample. $I(E_i)$ and $O(E_i)$ are the foreground counts for the sample in and out, $IB(E_i)$ and $OB(E_i)$ are the background counts for sample in and out, and M_I and M_O are monitor counts for the sample-in and the open beam, respectively. In this measurement, we assumed the monitor counts to be equal during the measurement.
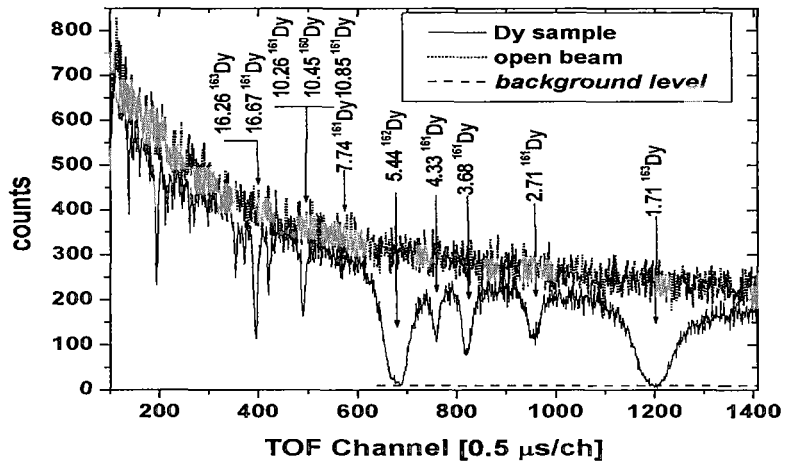
(a)
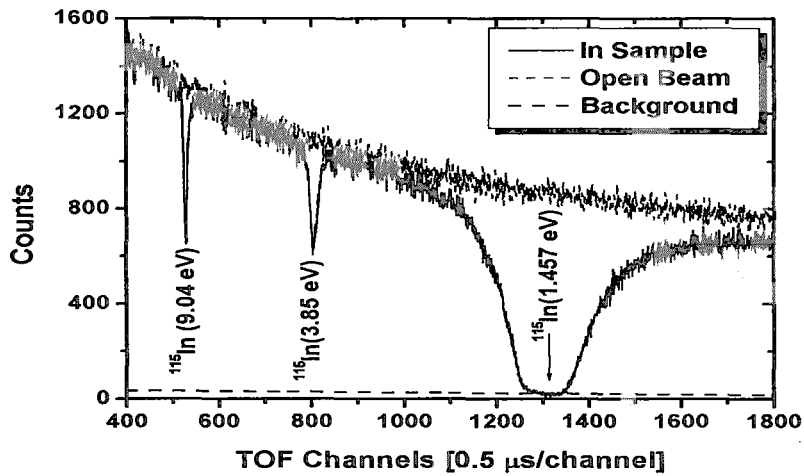
(b)
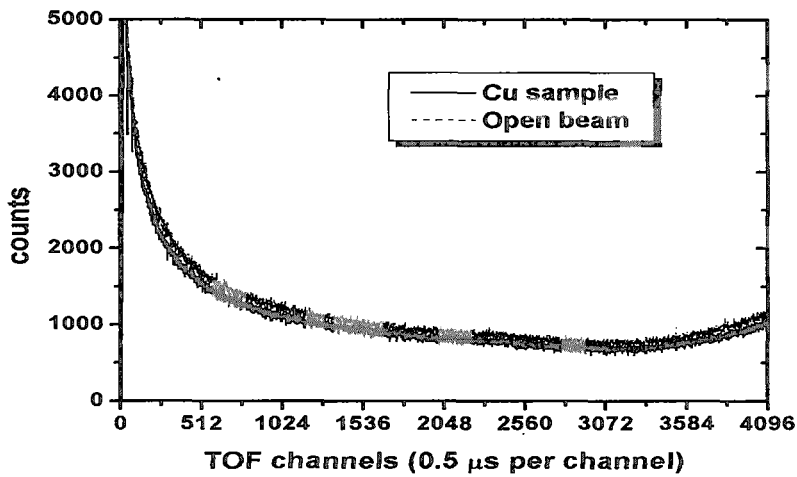
(c)

IV. RESULTS AND DISCUSSION

Fig.2. The net neutron TOF spectra for sample in and open beam of (a) Dy, (b) In, and (c) Cu samples.

The total cross-sections of natural Dy, In and Cu were obtained in the energy range from 0.1 eV to 100 eV by using the neutron TOF method. We only considered the statistical errors for the present measurements because the other sources of uncertainties, which include the detection efficiencies, the geometric factor for the sample, and the other systematic errors, are negligible. The present measurements for natural Dy, In and Cu are compared with the evaluated data in the ENDF/B-VI, as seen in Fig. 3, 4, and 5, respectively. The error bars in the figures indicate the statistical error only.
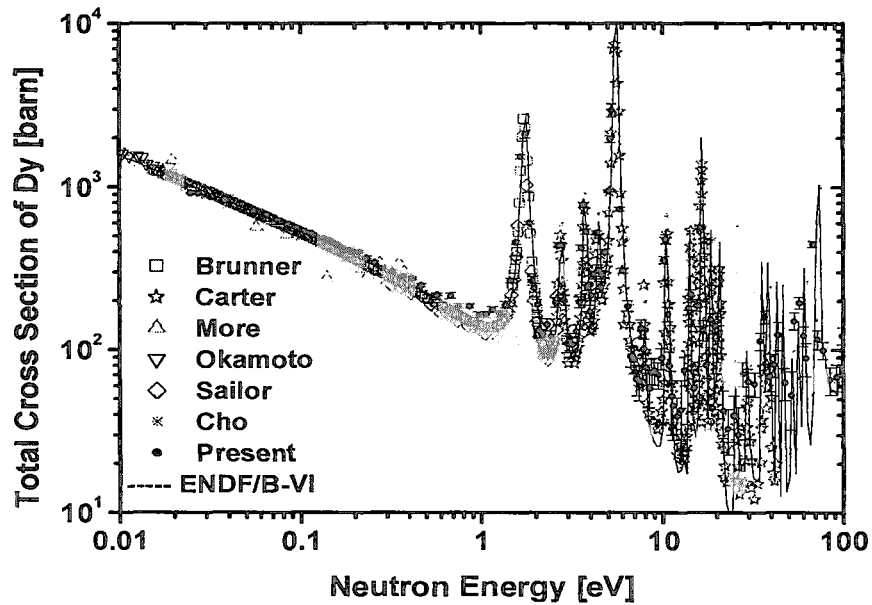

Fig. 3. Comparison of the measured neutron total cross-sections of natural Dy with the previous measurements and the evaluated data in ENDF/B-VI.
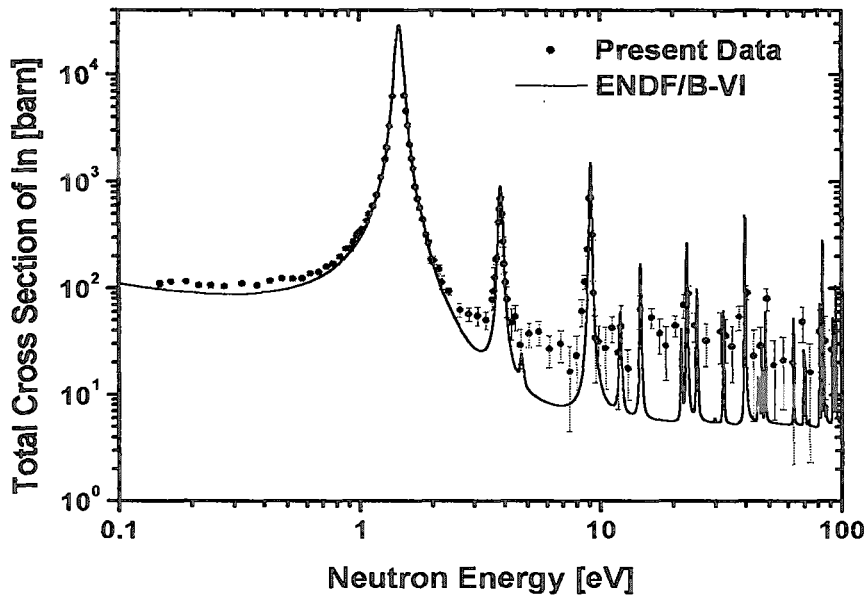

Fig. 4. Comparison of the measured neutron total cross-sections of natural In with the evaluated data in ENDF/B-VI.
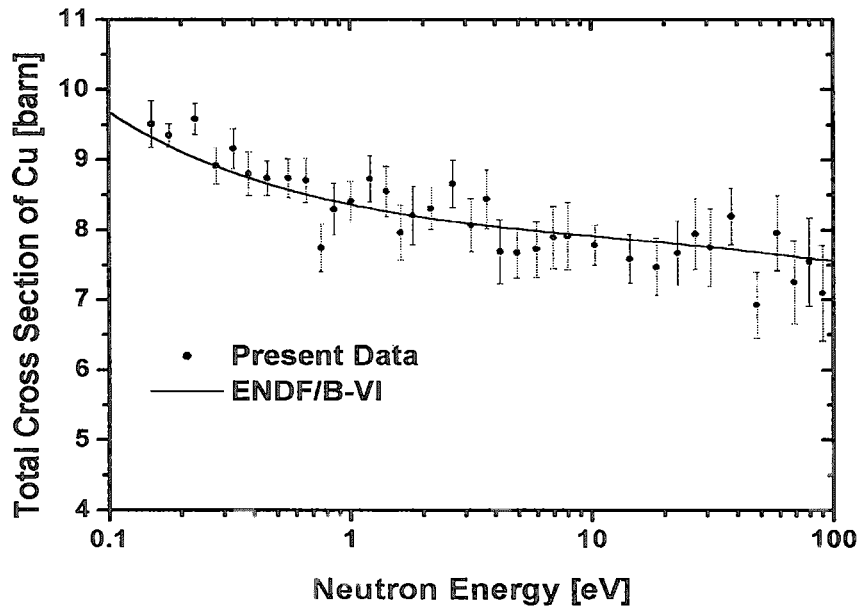
Fig. 5. Comparison of the measured neutron total cross-sections of natural Cu with the evaluated data in ENDF/B-VI.

The present measurement for the neutron total cross-sections of Dy is compared with other data measured by Moore [3], Okamoto [4], Sailor *et al.* [5], Brunner *et al.* [6], Knorr *et al.* [7], Carter [26], and Cho *et al.*[8] and the evaluated data in ENDF/B-VI [20]. The present measurement is generally in good agreement with other data and the evaluated one as shown in Fig. 3.

The present measurements for natural In and Cu are generally in good agreement with the evaluated data in ENDF/B-VI. The quality of these data is not good enough to compare with the previous measurements due to low statistics. The purpose of these measurements was to show the possibility of using the Pohang Neutron Facility equipped with the new data acquisition system as a nuclear data production facility.

There are several resonance peaks in the Dy total cross-sections. In order to get the resonance parameters of each resonance peak, we fit the transmission data with the SAMMY code [21]. This code uses the Reich-Moore approximation [27] in the application of the R-matrix formalism. An implementation of Bayes' theorem is used to fit the requested resonance parameters to the data. For the Doppler broadening and resolution analysis, the MULTI method [28] is applied: the free gas model is applied to the Doppler broadening and the convolution of Gaussian and exponential function to the resolution. Resolution function $R(E,E')$ used in this calculation is the convolution of Gaussian and exponential function and its mathematical expression is as follows:

$$R_{GE}(E,E') = \frac{1}{\Delta_E \Delta_G \sqrt{\pi}} \int_{E-\Delta E_S}^{\infty} dE^0 \exp\left\{-\frac{\left(E^0 - (E - \Delta E_S)\right)}{\Delta_E}\right\} \exp\left\{-\frac{\left(E'-E^0\right)^2}{\Delta_G^2}\right\}, \tag{3}$$

where the FWHM of Gaussian resolution function Δ_G is given by

$$\Delta_G = E[aE + b]^{1/2} \tag{4}$$

and the width of exponential resolution function Δ_E is given by

$$\Delta_E = cE^{3/2}.$$

(5)

The energy shift ΔE_S, which is automatically determined in SAMMY, is introduced in order that the maximum of the broadening function be located at $E' = E$. The constant values of a, b, and c are 1.3645×10^{-6} eV^{-1}, 9.1281×10^{-6}, and 6.3969×10^{-4} eV$^{-1/2}$, respectively.

Thus the resonance parameters, listed in Table 2, have been obtained from the resonance shape in transmission data and are compared with the set of data given between brackets [22]. Quantity J is the spin of a particular resonance. In Fig. 6, the measured total cross-section of Dy in the neutron energy range from 1 to 10 eV was compared with the SAMMY fitting results. The SAMMY prediction of total cross-section and the present data are in good agreement with each other with $\chi^2/N = 1.04$.

Table 2. Resonance Parameters for Dy isotopes

| Isotope	J	E (eV)		$g\Gamma_n$ (meV)	Γ_γ (meV)
^{163}Dy	2	Present	1.7093 ± 0.0007	0.9344 ± 0.0105	91.574 ± 0.827
		Mughabghab	(1.713 ± 0.004)	(0.85 ± 0.05)	(102.6 ± 0.8)
^{160}Dy	1/2	Present	1.8871 ± 0.0321	0.1394 ± 0.0135	124.97 ± 12.32
		Mughabghab	(1.88)	(0.20)	(105.80)
^{161}Dy	3	Present	2.6979 ± 0.0028	0.3929 ± 0.0122	130.12 ± 6.632
		Mughabghab	(2.71 ± 0.02)	(0.328 ± 0.015)	(119 ± 10)
^{161}Dy	2	Present	3.6618 ± 0.0025	0.9524 ± 0.0243	139.14 ± 6.087
		Mughabghab	(3.68 ± 0.03)	(0.89 ± 0.04)	(124 ± 15)
^{161}Dy	2	Present	4.2810 ± 0.0041	0.6677 ± 0.0273	130.25 ± 8.702
		Mughabghab	(4.33 ± 0.02)	(0.575 ± 0.065)	(80 ± 3)
^{162}Dy	1/2	Present	5.3697 ± 0.0022	14.492 ± 0.4007	262.08 ± 11.08
		Mughabghab	(5.44 ± 0.02)	(21 ± 1.5)	(148 ± 15)
^{163}Dy	2	Present	5.8377 ± 0.0775	0.0198 ± 0.0014	108.07 ± 10.81
		Mughabghab	(5.81)	(0.0135)	(108.60)
^{161}Dy	3	Present	7.6632 ± 0.0195	0.4284 ± 0.0340	158.01 ± 14.46
		Mughabghab	(7.74)	(0.30)	(107.00)
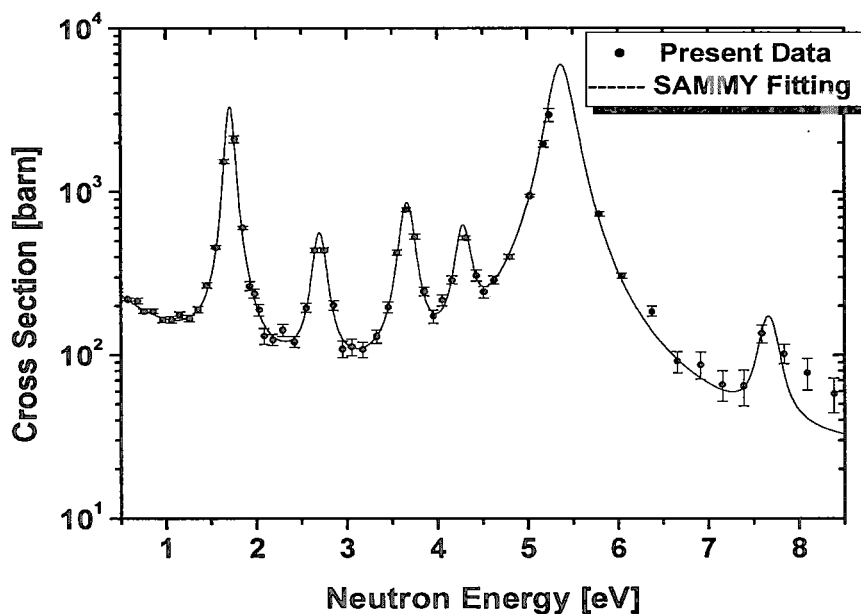
Fig. 6. Comparison of the measured total cross sections of natural Dy with the predicted total cross section from the SAMMY fitting

V. CONCLUSION

The Pohang Neutron Facility was constructed as a pulsed neutron facility based on an electron linac for producing nuclear data in Korea. It consists of a 100-MeV electron linac, a water cooled Ta target, and an 11-m long TOF path. In order to show the ability to measure nuclear data, we measured the neutron total cross-sections of natural Dy, In and Cu samples in the neutron energy range from 0.1 eV to 100 eV by using the neutron time-of-flight method with the new data acquisition system and a ^{6}LiZnS(Ag) glass scintillator as a neutron detector. The present measurements are in general agreement with the evaluated data in ENDF/B-VI. The resonance parameters of the Dy isotopes were extracted from the transmission rate compared with the previous ones.

Based on the present results, this pulsed neutron facility could be used as a user facility for nuclear data production. However, we have to upgrade the electron gun system for high current, wide pulse width, and high repetition rate, and we have to install a neutron monitor in front of the sample changer in order to monitor the neutron intensity. In order to decrease background events, we have to modify the shielding around the detector and the sample changer and add more collimators along the neutron beam tube. For the moment, we can measure the neutron total cross-sections only by using the neutron TOF method. In order to measure the neutron capture cross-sections, we have to construct a set of total energy absorption detectors employing BGO, NaI(Tl), or CsI(Tl).

ACKNOWLEDGMENTS

REFERENCES

[1] G. N. Kim, J. Y. Choi, M. H. Cho, I. S. Ko, W. Namkung, and J. H. Jang, in *Proceedings International Conference on Nuclear Data for Science and Technology*, edited by G. Reffo, A. Ventura and C. Grandi (Trieste, Italy, May 19-24, 1997), p. 556; H. S. Kang, J. Y. Choi, Y. J. Park, S. H. Kim, G. N. Kim, M. H. Cho, I.

S. Ko, and W. Namkung, in *Proceedings of First Asian Particle Accelerator Conference*, edited by Y. H. Chin, M. Kihara, H. Kobayashi, N. Akasaka, K. Nigorikawa, and M. Tobiyama (Tsukuba, Japan, Mar. 23-27, 1998), p. 743.

[2] G. N. Kim, Y. S. Lee, V. Skoy, V. Kovalchuk, M. H. Cho, I. S. Ko, W. Namkung, D. W. Lee, H. D. Kim, S. K. Ko, S. H. Park, D. S. Kim, T. I. Ro, and Y. G. Min, J. Korean Phys. Soc. **38**, 14 (2001); G. N. Kim, V. Kovalchuk, Y. S. Lee, V. Skoy, M. H. Cho, I. S. Ko, W. Namkung, D. W. Lee, H. D. Kim, S. K. Ko, S. H. Park, D. S. Kim, T. I. Ro, and Y. G. Min, Nucl. Instr. Meth. A **485**, 458 (2002).

[3] W. M. Moor, Bulletin of American Physical Society, **6**, 70 (1961).

[4] K. Okamoto, JAERI Report, JAERI-1069 (1964).

[5] V. L. Sailor, H. H. Landon, and H. L. Jr. Foot, Phys. Rev. **96**, 1014 (1954).

[6] J. Brunner and F. Widder, Report EIR-123 (1967).

[7] K. Knorr and W. Schmatz, Atomk-ernenergie **16** (9), 49 (1970).

[8] H. J. Cho, K. Kobayashi, S. Yamamoto, Y. Fujita, Y. S. Lee, G. N. Kim, I. S. Ko, M. H. Cho, W. Namkung, S. K. Ko, Annals of Nuclear Energy, **27**, 1259 (2000).

[9] K. K. Seth, D. J. Hughes, R. L. Zimmerman, and R. C. Garth, Phys. Rev. C **110**, 692 (1958).

[10] M. S. Pandey, G. B. Garg, and J. A. Harvey, Phys. Rev. C **15**, 600 (1977).

[11] R. G. Allen, T. E. Strephenson, C. P. Stanford, and S. Bernstein, Phys. Rev. **96**, 1297 (1954).

[12] H. H. Landon and V. L. Sallor, Phys. Rev. **98**, 1267 (1955).

[13] W. W. Havens JR. and J. Rainwater, Phys. Rev. **73**, 963 (1948).

[14] J. A. Harvey, D. J. Hughes, R. S. Cater and V. E. Pilcher, Phys. Rev. **99**, 443 (1955).

[15] R. F. Bacher, C. P. Baker, and B. D. McDaniel, Phys. Rev. **69**, 165 (1946).

[16] W. W. Havens, Jr., C. S. Wu, L. J. Rainwater, and C. L Meaker, Phys. Rev. **71**, 165 (1947).

[17] D. Boyce and McDaniel, Phys. Rev. **70**, 832 (1946).

[18] G. Hacken, H. I. Liou, H. S. Camarda, W. J. Makofske, F. Rahn, L. J. Rainwater, M. Slgawitz, and S. Wynchank, Phys. Rev C **10**, 1910 (1974).

[19] C. M. Frankle, J. D. Dawman, B. E. Crawford, P. P. J. Delheij, C. R. Gould, D. G. Hase, J. N. Knudson, G. E. Mirchel, S. S. Patterson, S. I. Penttila, Yu. P. Popov, N. R. Roberson, S. J. Seestrom, E. I. Sharapov, Yi. Fen Yen, S. H. Yoo, V. W. Yuan, and X. Zhu Phys. Rev, C **48**, 1601 (1993).

[20] R. F. Ross, ENDF-201, ENDF/B-VI Summary Documentation, BNL-NCS-17541, 4th Ed. (ENDF/B-VI), Brookhaven National Laboratory (1991).

[21] N. M. Larson, RSICC Peripheral Shielding Routine Collection SAMMY-M2a: A Code System for Multilevel R-Matrix Fits to Neutron Data Using Bayes' Equations, PSR-158, SAMMY-M2a, Oak Ridge National Laboratory (1999) (unpublished).

[22] S. F. Mughabghab, Neutron Cross-sections (Academic Press, NY, 1984) Vol. 1.

[23] W. Y. Baek, G. N. Kim, M. H. Cho, I. S. Ko, and W. Namkung, in Proceedings of Workshop on Nuclear Data Production and Evaluation, edited by J. Chang and G. N. Kim (Pohang, Korea, Aug. 7-8, 1998).

[24] MCNP, A general Monte Carlo N-Particle transport code system, Version 4B, Los Alamos National Laboratory, LA-12625-M, (1997).

[25] V. Skoy, Y. S. Lee, H. S. Kang, M. H. Cho, I. S. Ko, W. Namkung, G. N. Kim, R. Machrafi, H. Ahmed, and D. Son, J. Korean Phys. Soc., **41**, 314 (2002).

[26] R. S. Carter, Exfor Data File 11897 (1983).

[27] C. W. Reich and M. S. Moore, Phys. Rev. **111**, 929 (1958).

[28] F. A. George, "MULTI, A FORTRAN Code for Least-Square Shape Fitting of Neutron Cross-Section Data Using the Reich-Moore Multilevel Formalism," LA-5473-MS, Los Alamos Scientific Laboratory (1974).